

Classical study of $p + \text{He}$ and $p + \text{He}^+$ collisions in intense laser fields

L. Feng^{1,a} and Y.-k. Ho^{2,1,b}¹ Institute of Modern Physics, Fudan University, Shanghai 200433, China² CCAST (World Laboratory), P.O. Box 8730, Beijing 100080, China

Received: 7 October 1998 / Received in final form: 28 January 1999

Abstract. In this paper, ion-atom and ion-ion collisions in the presence of intense laser fields are qualitatively studied by Classical Trajectory Monte Carlo (CTMC) simulations. It is found that in contrast to the field-free collisions, the colliding ion and the target nucleus could absorb energy from the applied laser fields when the electrons escape from the collision system. This result is explained in terms of Coulomb explosion induced by the enhanced ionization at the so-called critical internuclear distance. Also, the corresponding energy gain cross-sections are evaluated.

PACS. 33.80.Rv Multiphoton ionization and excitation to highly excited states (e.g., Rydberg states) – 34.10.+x General theories and models of atomic and molecular collisions and interactions (including statistical theories, transition state, stochastic and trajectory models, etc.) – 34.50.Fa Electronic excitation and ionization of atoms (including beam-foil excitation and ionization)

1 Introduction

Recently, many theoretical and experimental researches are devoted to the dissociation ionization of molecules by intense laser fields [1–7]. Those studies reveal that the laser ionization of diatomic molecules can be greatly enhanced, compared with that of atoms. For example, D. Normand and M. Schmidt [5] found that up to ten electrons can be removed from the iodine molecule by an intense laser beam with intensity $1.3 \times 10^{14} \text{ W/cm}^2$, while the same laser field cannot extract three electrons from the iodine atom. This interesting result has been explained in terms of the enhanced ionization at the so-called critical internuclear distance [4–7].

Thus, it may be expected that for ion-atom (or ion-ion) collisions in intense laser fields, the laser ionizations would be enhanced when the separation between the projectile and target reaches the vicinity of the critical internuclear distance. This idea is schematically shown in Figure 1, where the potentials experienced by an electron moving along the axis between the target nucleus and the incident projectile are drawn for two typical cases: one where the internuclear separation is greatly larger than the critical internuclear distance and the other where the internuclear separation is close to the critical internuclear distance. In each curve there are two potential wells centered at the target nucleus and the positive-charged projectile, respectively. At the beginning, the electron is bound in the left

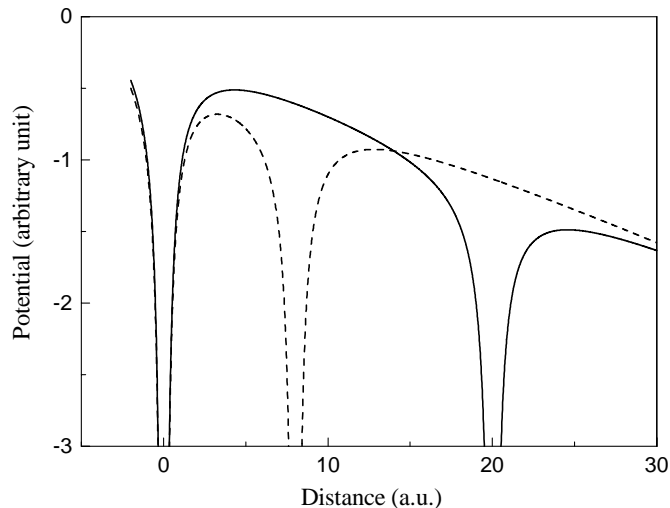


Fig. 1. The schematic draw of the potentials experienced by an electron moving in the combined field of the projectile, atomic nucleus as well as the applied laser field. The solid line corresponds to the large internuclear separation, and the dashed line is for the intermediate internuclear separation.

well generated by the target nucleus. When the internuclear separation is large (corresponding to the solid line in Fig. 1), although distorted by the applied laser field, the barrier of the atomic potential well is still too high for the electron to overcome, and thus, the atom will not be seriously ionized. But, when the projectile moves closer (the dashed line in Fig. 1), the inner barrier between the

^a e-mail: lngfeng@fudan.ac.cn^b e-mail: hoyk@fudan.ac.cn

two potential wells becomes lower, and thus, the electron is able to pass through the inner barrier and escape from the system directly. Furthermore, this abrupt ionization will result in an increase of the total kinetic energy of the projectile and the target nucleus by an amount $\sim 1/R_{\text{ion}}$ (atomic units are adopted throughout this paper), where R_{ion} denotes the internuclear separation at which the ionization takes place. This mechanism is of practical interest, since by it the colliding particles, which are much heavier than electrons, can directly absorb energy from the applied laser field.

The main purpose of this paper is to show this energy absorption mechanism by Classical Trajectory Monte Carlo (CTMC) simulations. Here, $p + \text{He}$ and $p + \text{He}^+$ collisions are chosen as the examples of ion-atom and ion-ion collisions, respectively. In the second section, we briefly describe the theoretical model of the CTMC simulation. In the third section, numerical results for $p + \text{He}$ collisions in intense laser fields are presented. Here, one can see that the Coulomb explosion, which is induced by the enhanced ionization in the vicinity of the critical internuclear distance, can result in an increase of the kinetic energy of the colliding particles. In the fourth section, similar calculations are performed for $p + \text{He}^+$ collisions. Also, in this section, a comparison is made between $p + \text{He}^+$ and $p + \text{He}$ collisions. Finally, the fifth section includes a simple conclusion.

2 Theoretical model

In principle, ion-atom collisions should be treated by quantum mechanics. However, a full quantum treatment is quite difficult, especially for the processes in which many active particles are involved in energy exchange. An alternative way is the so-called CTMC simulation, where an ensemble of classical particle trajectories with randomly selected initial conditions are calculated in the frame of classical dynamics, and the physical results are obtained by averaging over those trajectories. The CTMC method has been successfully applied to investigate field-free ion-atom collisions at the intermediate collision energy region [8]. It has also been extended to study the collisions between the Rydberg atoms and the slow singly charged ions (the collision energy is as low as 1.3 eV/amu) [9]. In fact, the classical models are also frequently used to study the responses of atoms and molecules to intense laser fields [6, 10–12], since when an atom (or a molecule) is irradiated by an intense laser field, its electronic structure will be strongly distorted, and the increase of the classical behavior of the quantum system is expected. So, the CTMC method is suitable to provide us with a simple qualitative description of the atom-ion (or ion-ion) collisions in an intense laser field.

In the presence of an intense laser field, the Hamiltonian for the system formed by a target atom (ion) with N_e electrons and an incident proton is given by (in atomic units)

$$H = T_{\text{ap}} + V_{\text{ap}} + \varepsilon_e + V_{\text{ext}}. \quad (1)$$

Here, the total kinetic energy of the target nucleus and incident proton is

$$T_{\text{ap}} = \frac{\mathbf{P}_a^2}{2m_a} + \frac{\mathbf{P}_p^2}{2m_p}, \quad (2)$$

where the indices a and p denote the target nucleus and the projectile, respectively. V_{ap} is the Coulomb interaction between the target nucleus and the incident projectile, *i.e.*

$$V_{\text{ap}} = \frac{Z_a Z_p}{|\mathbf{R}_a - \mathbf{R}_p|}, \quad (3)$$

where Z_a and Z_p are the charge of the target nucleus and the projectile, respectively, and \mathbf{R}_a and \mathbf{R}_p represent their positions. The energy of the electrons in the target is calculated by

$$\varepsilon_e = \sum_{i=1}^{N_e} \frac{\mathbf{P}_{ei}^2}{2} + V_{\text{Coul}}, \quad (4)$$

where \mathbf{P}_{ei} denotes the momentum of the i -th electron, and the Coulomb potential V_{Coul} is given by

$$V_{\text{Coul}} = - \sum_{k=a,p} \sum_{i=1}^{N_e} \frac{Z_k}{\left[|\mathbf{R}_k - \mathbf{r}_i|^2 + \alpha^2\right]^{1/2}} + \sum_{i>j}^{N_e} \frac{1}{\left[|\mathbf{r}_i - \mathbf{r}_j|^2 + \alpha^2\right]^{1/2}}. \quad (5)$$

Here, \mathbf{r}_i is the position of the i -th electron. Note that a smearing parameter α is introduced to remove the singularity of the Coulomb interaction. The introduction of a smearing parameter α to the standard Coulomb interaction is not only a mathematical trick to avoid numerical problem, but it can also be considered as the result of Heisenberg uncertainty relation [6]. In our present simulations, α is chosen to be equal to 1.0.

The interaction between the collision system and the applied laser field $\mathbf{E}(t)$ is given by

$$V_{\text{ext}} = - \sum_{k=a,p} Z_k \mathbf{E}(t) \cdot \mathbf{R}_k + \sum_{i=1}^{N_e} \mathbf{E}(t) \cdot \mathbf{r}_i, \quad (6)$$

where

$$\mathbf{E}(t) = E_0 U(t) \sin(\omega t + \beta) \hat{z}. \quad (7)$$

Here, E_0 is the amplitude of the laser electric field, ω is the frequency, and β is the initial phase. The envelope of the laser pulse is represented by $U(t)$ in the following form:

$$U(t) = \left\{ \begin{array}{ll} t/\tau_p, & 0 < t < \tau_p \\ 1, & \tau_p < t < 11\tau_p \\ (12\tau_p - t)/\tau_p, & 11\tau_p < t < 12\tau_p \\ 0, & t > 12\tau_p \end{array} \right\}. \quad (8)$$

So, the laser pulse has a distinct starting and stopping time, and remains mostly uniform for the pulse duration.

For the first step of CTMC calculations, an ensemble of initial conditions of the collision system should be given. For both p + He and p + He⁺ collisions, the following assumptions are made: 1) at $t = 0$, the separation between the projectile and target is equal to 50 a.u., and they move towards each other along the direction of the laser electric field. Also, the magnitude of the initial momentum of the target nucleus is chosen to be equal to that of the projectile momentum. 2) the target is in its ground state before the laser field is turned on. In the present simulations, the sampling of the initial configurations of the target is made by two different approaches, which are demonstrated in detail in Section 3 and Section 4, respectively. The impact parameter b is chosen by uniform sampling of $b^2 \in [0, b_{\max}^2]$. Note that at the moment when the laser field is turned on, the incident protons lie in various distances from the targets, and therefore, enter the collision region at different laser field phases. This condition is taken into account by randomizing β , the initial phase of the laser pulse.

With a selected initial configuration, each classical trajectory of the collision system is given by numerical integration of the Hamiltonian equations. Here, the Runge-Kutta method with variable step sizes is adopted to perform numerical integrations. The accuracy of the integrations is verified by the energy conservation during the field-free p + He⁺ and p + He collisions. It is found that the law of energy conservation is fulfilled to an accuracy of 10^{-4} .

3 ion-atom collision in intense laser fields

In this section, we will discuss the p + He collisions in the presence of an intense laser field. Normally, a classical multielectron atom is unstable even if no external field is applied, since one electron can absorb sufficient energy to escape from the atom by pushing other electrons to deeply bound states. However, in the case of smooth Coulomb potential, two-electron atom would be stable provided that the ground-state energy is chosen to be sufficiently low [12]. In our simulations, the helium atom is modeled with ground-state energy of -2.9 a.u., and it is stable without external fields. Generally, the assemble of the initial configuration of the helium atom cannot be generated by the method widely used for the atoms with one active electron [10]. Here, we trace the time evolution of the two electrons in the helium atom, and select the states at the randomly chosen instants as the initial configurations [6,12]. The initial total kinetic energy of the target nucleus and the projectile is chosen to be $T_{\text{ap}} = 0.2$ a.u. Obviously, the incident energy of the collision system is corresponding to a temperature of several ten thousand kelvins. The parameters of the applied laser field are chosen as $E_0 = 0.24$ a.u. (corresponding to the laser intensity 2×10^{15} W/cm²), $\omega = 0.043$ a.u. (Nd Laser), and $\tau_p = 600$ a.u. Note that without the incident proton, about 7.2% of the model helium atom would be ionized by such a

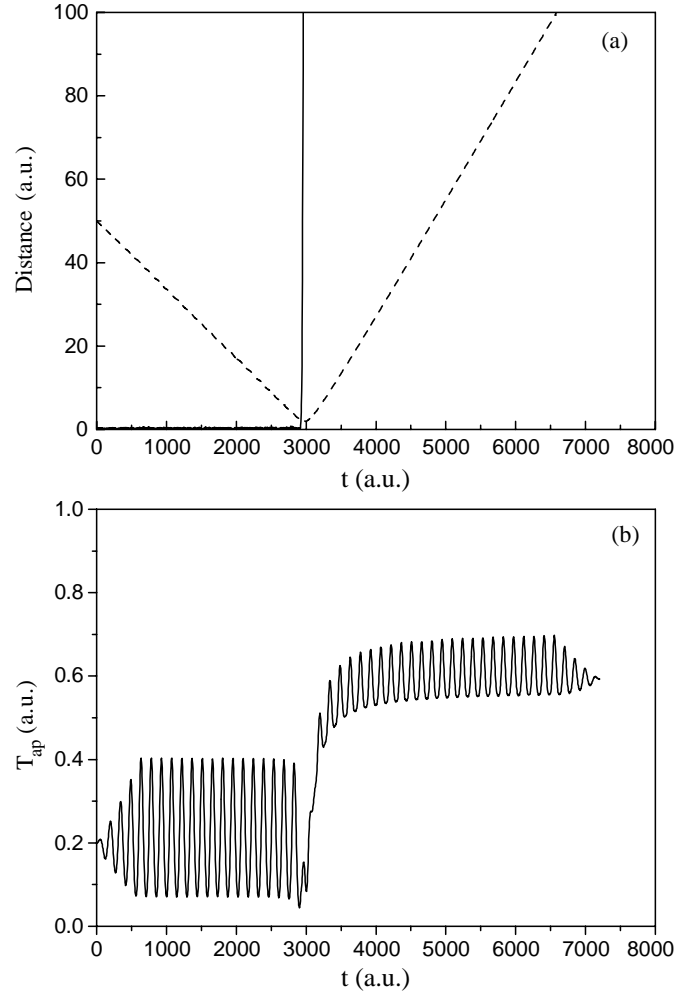


Fig. 2. Temporal evolutions of a typical trajectory of p + He collisions in an intense laser field with intensity 2×10^{15} W/cm². Here, the initial total kinetic energy of the incident proton and the target nucleus is equal to 0.2 a.u., and the impact parameter b is 1.5 a.u. (a) The time evolutions of the distance of the ionized electron to the atomic nucleus (the solid line) r_a , and the internuclear separation R_{ap} (the dashed line); (b) the time evolution of the total kinetic energy T_{ap} .

laser pulse. Note that the classical atoms with the smeared Coulomb potential are more stable than reality, and their ionization probabilities are underestimated [6,13].

Now, we turn to discuss the p + He collisions in this intense laser field. At first, the time evolution of a typical trajectory in which one electron is ionized is presented in Figure 2. In Figure 2(a), the distance of the ionized electron from the atomic nucleus $r_a = |\mathbf{r}_1 - \mathbf{R}_a|$ (the solid line) and the internuclear separation $R_{\text{ap}} = |\mathbf{R}_a - \mathbf{R}_p|$ (the dashed line) are shown as a function of time. Figure 2(b) plots the time evolution of the total kinetic energy T_{ap} . It can be seen that the electron stands against ionization until $t \sim 2500$ a.u., although the applied laser intensity has reached its maximum for some time. However, when the internuclear separation is reduced to about 2.5 a.u. at $t \sim 3000$ a.u., the electron feels a strong attrac-

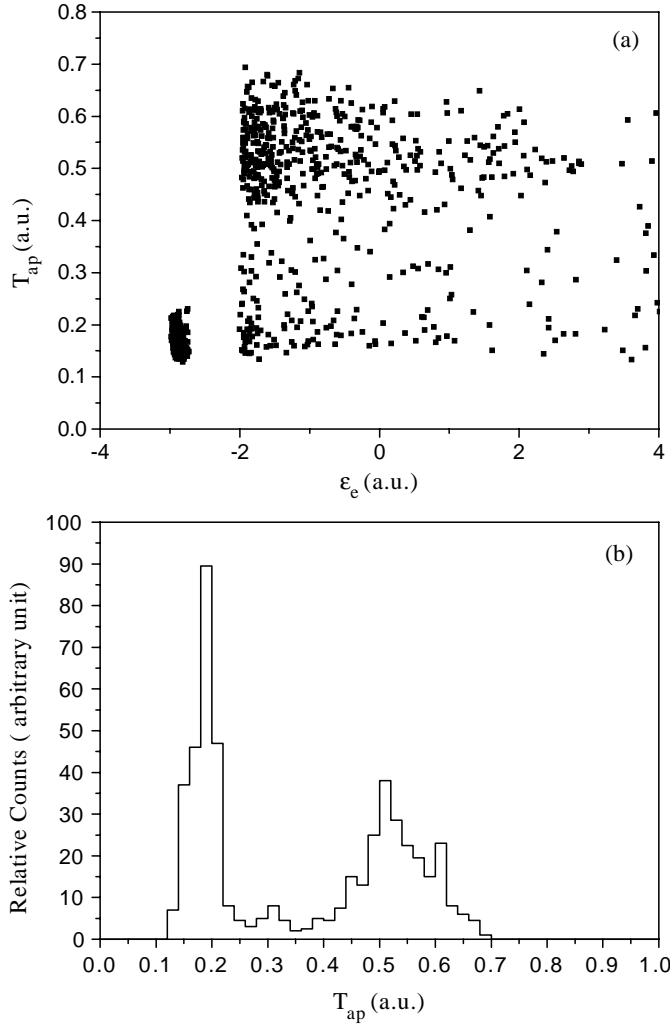


Fig. 3. The change of the total kinetic energy T_{ap} during p+He collisions in the presence of an intense laser field. The parameters of the applied laser field are the same as in Figure 2. Here, a total of $N = 2500$ trajectories with impact parameter b chosen by uniform sampling of $b^2 \in [0, b_{\text{max}}^2]$ ($b_{\text{max}} = 2.0$ a.u.) are calculated. (a) The correlation between the final electron energy ε_e and the final total kinetic energy T_{ap} ; (b) the spectrum of the final total kinetic energy T_{ap} .

tion from the approaching proton, and finally escapes from the system (see the solid line). Associated with this rapid ionization is an increase of the total kinetic energy T_{ap} , which could be observed in Figure 2(b). Note that the kinetic energy gain in this collision is about $\Delta T_{\text{ap}} \sim 0.4$ a.u., and can be related to the internuclear distance R_{ion} where the ionization takes place by the relation $\Delta T_{\text{ap}} \sim 1/R_{\text{ion}}$. This observation supports our above qualitative discussions.

To examine this ionization scheme more thoroughly, for the same laser field as in Figure 2, we calculate a total of $N = 2500$ trajectories with the randomly chosen initial target atom configurations and impact parameters. Here, the maximum impact parameter b_{max} is chosen to be 2.0 a.u. In Figure 3(a), T_{ap} is plotted *vs.* the final elec-

tron energy ε_e . Note that all the final states lie in two regions, which are separated by a gap in the electron energy with a width $\delta\varepsilon_e \sim 1.0$ a.u. In the first region with $\varepsilon_e < -0.2$ a.u., both electrons remain bound after the collisions, while the corresponding final total kinetic energy T_{ap} spreads around its initial value (0.2 a.u.). Note that in this region, no obvious energy gain is observed. In contrast, in the second region ($\varepsilon_e > -0.2$ a.u.), where one electron is ionized, T_{ap} is much larger than its initial value. The spectrum of the final total kinetic energy T_{ap} is plotted in Figure 3(b). Note that there are two separate peaks around $T_{\text{ap}} \sim 0.20$ a.u. and $T_{\text{ap}} \sim 0.55$ a.u., respectively. The first peak corresponds to the first region in Figure 3(a), and the second peak corresponds to the trajectories with electron ionization. Also, from Figure 3, it can be inferred that most of the ionizations take place just when the internuclear separations are in the range of 2.0 to 4.0 a.u.

The above discussion shows a basic feature of the ion-atom collisions in the presence of an intense laser, namely, the ionization of the target atom is accompanied by an increase in the total kinetic energy T_{ap} . So, the corresponding energy gain cross-sections are calculated by

$$\Delta T_{\text{ap}}\sigma = \pi b_{\text{max}}^2 \frac{1}{N} \sum_i \Delta T_{\text{ap}}(i), \quad (9)$$

where N is the number of the sample trajectories, and $\Delta T_{\text{ap}}(i)$ denotes the kinetic energy gain associated with the i -th trajectory. The upper limit of the impact parameters, b_{max} , is chosen to be large enough to ensure that the energy gain cross-sections are not b_{max} dependent. Finally, for $b_{\text{max}} = 3.0$ a.u. and $N = 5000$, we get that $\Delta T_{\text{pp}}\sigma = 3 \times 10^{-15}$ eV cm². It is instructive to compare the present results with the inverse bremsstrahlung absorption of laser fields. From equation (64) in reference [14], the averaged energy gain cross-section for the inverse bremsstrahlung absorption can be evaluated by (in atomic units)

$$\overline{\Delta\varepsilon_{\text{th}}\sigma} = \frac{dW/dt}{n_p \sqrt{2\varepsilon_{\text{th}}}} = \frac{8\omega}{E_0 \sqrt{2\varepsilon_{\text{th}}}} \ln\left(\frac{2\varepsilon_{\text{th}}}{3\omega}\right) \ln\left(\frac{E_0}{\omega \sqrt{2\varepsilon_{\text{th}}/3}}\right), \quad (10)$$

where n_p is the density of protons, ε_{th} is the electron thermal energy. Thus, for $\varepsilon_{\text{th}} = 0.20$ a.u. and $E_0 = 0.24$ a.u., $\overline{\Delta\varepsilon_{\text{th}}\sigma}$ is approximately 5×10^{-15} eV cm², which is of the same order of magnitude compared with that of the mechanism discussed in the present paper. Due to the fact that the mean electron velocity is much higher than the ionic velocity, the energy absorbed by this mechanism is only a few percent of that by inverse bremsstrahlung. However, in the present mechanism, the energies of the laser field are directly transferred to the heavy particles instead of the free electrons.

In the last decade, the electron collective response to the intense laser has been a major topic of many theoretical and experimental researches. To show whether the collective ionization can be observed in p + He collisions,

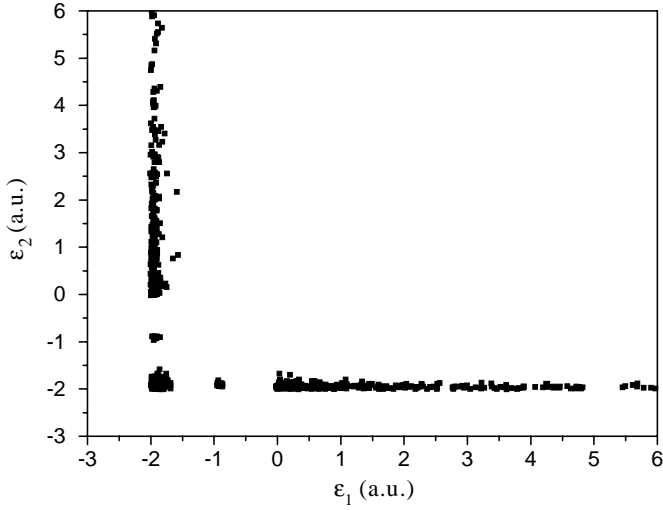


Fig. 4. The correlation between the two target electrons in p + He collisions in an intense laser field with intensity $2 \times 10^{15} \text{ W/cm}^2$.

we plot the final energy of one electron ε_1 *vs.* that of another ε_2 in Figure 4. Here, the final energy of the i -th electron is calculated by

$$\varepsilon_i = \frac{1}{2} \mathbf{P}_{ei}^2 - \frac{Z_a}{[(\mathbf{r}_i - \mathbf{R}_a)^2 + \alpha^2]^{1/2}} - \frac{Z_p}{[(\mathbf{r}_i - \mathbf{R}_p)^2 + \alpha^2]^{1/2}}. \quad (11)$$

Obviously, there is nearly no trajectory where the two electrons are ionized together, and thus no collective ionization could be observed in our cases.

4 ion+ion collision in an intense laser field

We now turn to discuss p + He⁺ collisions in an intense laser field. Due to the repulsive interaction between the positive-charged helium ion and the proton, additional kinetic energy is needed for them to reach the critical internuclear distance. Because the electron in He⁺ is quite deeply bound, a stronger laser field is also necessary. For the initial total kinetic energy $T_{\text{ap}} = 0.75$ a.u. and laser intensity $9 \times 10^{15} \text{ W/cm}^2$, a total of $N = 2500$ trajectories with the randomly selected initial configurations are calculated. Here, the maximum impact parameter b_{max} is equal to 2.0 a.u. The ground-state energy of He⁺ is chosen to be -2.0 a.u., and the corresponding microcanonical distribution of the target electron is given by the widely used approach [7, 10]. In Figure 5(a), the final total kinetic energy T_{ap} is plotted *vs.* the electron energy ε_e . Just as what we have observed in Figure 3, the trajectories spread in two regions in the $T_{\text{ap}}-\varepsilon_e$ space. One corresponds to the trajectories with electron ionization, and the other is for those without ionization. In Figure 5(b), the corresponding spectrum of the final total kinetic energy T_{ap} is presented. Here, one can also find two separate peaks, which shows that in intense laser fields, collisions between ions

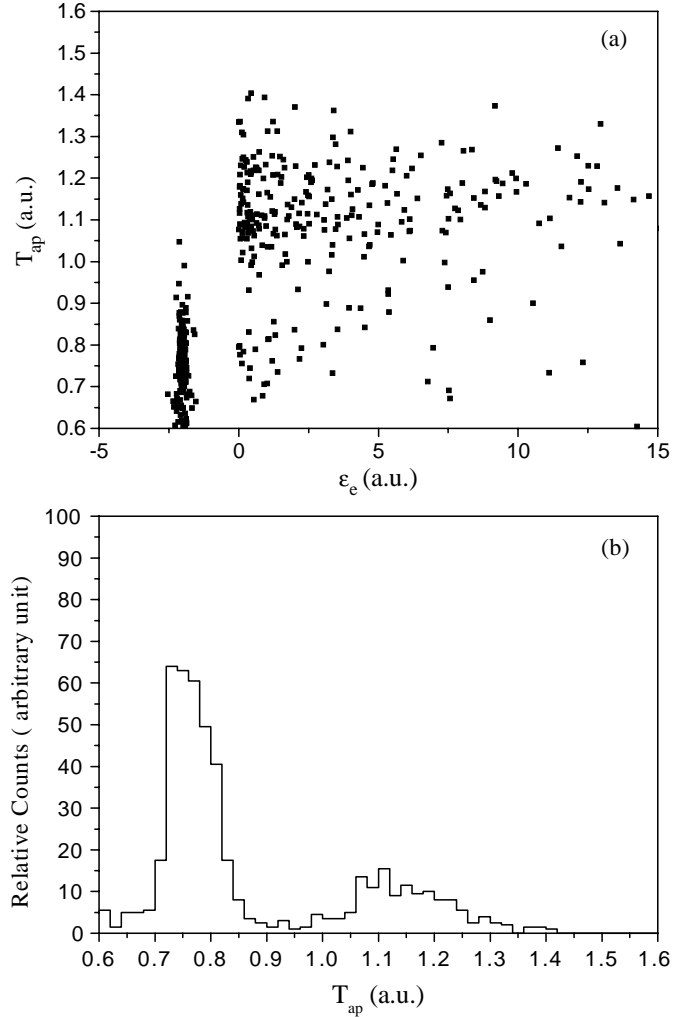


Fig. 5. The same as Figure 3 but for p + He⁺ collisions. Here, the initial total kinetic energy T_{ap} is 0.75 a.u., and the laser intensity is $9 \times 10^{15} \text{ W/cm}^2$.

and ions can result in an increase of the kinetic energy of the colliding particles.

However, compared with p + He collisions, fewer trajectories lead to electron ionization, although the applied laser is much stronger. Partly, this result is due to the repulsion between the projectile and the target which makes it hard for the projectile and the target to get sufficiently close to each other.

5 Summary

In conclusion, p + He⁺ and p + He collisions in an intense laser field are qualitatively investigated by CTMC simulations. It is found that those collisions can lead to an increase in the ionic kinetic energies. This observation can be interpreted in terms of the enhanced ionization in the vicinity of the critical internuclear separation. This new energy absorption mechanism is of practical interest, since the colliding particles, which are much heavier than

electrons, can be directly heated by the applied intense laser fields.

There are many questions left open for future studies. For example, in the present CTMC simulations, the quantum effects such as the tunneling ionization and the molecular states during the ion-atom collisions in intense laser fields are ignored. We plan to discuss these questions in future papers.

This work is partly supported by Project 19804002 of NSFC, the National High-Tech ICP Committee in China, the Natural Science Foundation of Shanghai Education Department and the Natural Science Foundation of Fudan University.

References

1. C. Cornaggia, D. Normand, J. Morellec, *J. Phys. B* **25**, L415 (1992).
2. M. Brewczyk, K. Rzazewski, C.W. Clark, *Phys. Rev. Lett.* **78**, 191 (1997).
3. K. Codling, L.J. Frasinski, *J. Phys. B* **26**, 783 (1993).
4. S. Chelkowski, A. Conjusteau, T. Zuo, A.D. Bandrauk, *Phys. Rev. A* **54**, 3235 (1996).
5. D. Normand, M. Schmidt, *Phys. Rev. A* **53**, R1958 (1996).
6. D.M. Villeneuve, M.Yu. Ivanov, P.B. Corkum, *Phys. Rev. A* **54**, 736 (1996).
7. E. Constant, H. Stapelfeldt, P.B. Corkum, *Phys. Rev. Lett.* **76**, 4140 (1996).
8. R. Abrines, I.C. Percival, *Proc. Phys. Soc. Lond.* **88**, 861 (1966).
9. S. Bradenbrink, E.Y. Sidiy, Z. Roller-Lutz, H. Reihl, H.O. Lutz, *Phys. Rev. A* **55**, 4290 (1997).
10. G. Bandarage, A. Maquet, J. Cooper, *Phys. Rev. A* **41**, 1774 (1990).
11. M. Gajda, J. Grochmalicki, M. Lewenstein, K. Rzazewski, *Phys. Rev. A* **46**, 1638 (1992).
12. K. Rzazewski, M. Lewenstein, P. Salieres, *Phys. Rev. A* **49**, 1196 (1994).
13. B. Walker, B. Sheehy, L.F. DiMauro, P. Agostini, K.J. Schafer, K.C. Kulander, *Phys. Rev. Lett.* **73**, 1227 (1994).
14. D. Jones, K. Lee, *Phys. Fluids* **25**, 2307 (1982).